# Numerical simulation of water freezing in low temperature reservoir of a heat pump

Hugo Ksawery Urbańczyk

hugourbanczyk1@gmail.com

Instituto Superior Técnico, Universidade de Lisboa, Portugal

November 2022

## Abstract

This work presents numerical simulations of water freezing around an exemplary, horizontal pipe that could be used in a water tank being the temperature reservoir of a heat pump installation. This type of installation is a relatively new and developing concept of *ice heating*, which allows in a winter to collect significant amount of heat from water and causes it to freeze. This allows to use the frozen water in the summer as a sink of surplus heat. The aim of the work was to determine the quantitative and qualitative nature of freezing under various conditions that may occur in a water tank as the freezing in that type of installation has many constraints.
The simulations were carried out in the Ansys Fluent 2022 R1 software with use of *Solidification and Melting* module. Two numerical cases were designed - steady simulation of glycol flow through the pipe in 3D and transient simulation of water freezing around cross section of the pipe in 2D. The first case allowed to identify the glycol flow properties while the second tested the rate and characteristics of freezing. The obtained results allowed to determine the lower time limit of freezing the finite volume of water and to assess the impact of the choice of pipe material. Additionally, the pipe lengths necessary to obtain 1 kW of power were determined. Finally, recommendations were formulated for those who would like to investigate the topic in the future.

**Key words:** ice heating, water freezing, numerical simulation, heat pump, solidification, phase change

## 1. Introduction

Heat pumps are now becoming an increasingly popular and promoting solution in the field of individual heating, mainly in single-family houses. This leads to an increasing demand for electricity and the risk of overloading power grids. The heat pump is a very convenient solution as it does not require any specialist knowledge from the user, or any noticeable effort to operate. It does not emit pollutants into the atmosphere, so it might be called as an ecological source of heat.
In the era of progressing electrification, people more and more often decide to change the classic heating systems (powered by solid, or liquid fuels) to heat pumps. To maintain positive trend of heat source replacement while understanding and respecting the need to improve thermal comfort in buildings, it is irrecusably important to try to improve the operation of heating and cooling systems.
In this study, the analyzed configuration is a water heat pump with the lower heat source being a closed, artificial water tank, while the working medium is a mixture of water and ethylene glycol [1,2]. The adopted water heat pump solution can be improved in such a way as to lead to a controlled freezing of the water in the tank. This is called *Ice Heating* and allows to achieve two substantial benefits:

- Utilization of latent heat of water $3.34*10^5$ J/kg [3]
- Use of ice accumulated during winter for cooling purposes in the summer.

Storing the cool for summer while heating in winter seems to be a simple and brilliant idea – so why is it not a commonly used solution? Several major obstacles can be cited; however, the biggest problem is the complex nature of the freezing process forcing a specialized heat exchanger design in this tank. At present, only a few (mainly German) companies in Europe undertake the construction of ice heating installations, probably diligently protecting their know-how. In such circumstances, it is justified to investigate how the water freezing process in the water tank occurs and to determine how the low temperature heat exchanger should be designed to ensure failure-free and efficient operation.

## 2. Objectives

The aim of the work is numerical modeling of water freezing around an exemplary pipe from which a heat exchanger could probably be made. The work is therefore focused on assessing the course of the phenomenon occurring in a specific location of the heat pump installation

It was decided to create two numerical cases. The first, a steady simulation of glycol flowing through a pipe in 3D was to determine: velocity profile of in the pipe; the heat transfer coefficient (HTC) between the glycol and the pipe inner wall; and the glycol temperature increase along the pipe length.

Due to the limited computational capacities, simulation of freezing was performed as 2D simulation of cross section of the horizontally oriented pipe. Several variants were prepared – with different initial temperatures and with or without mass exchange at the boundaries of the computational domain. These simulations were to: determine ice growth rate in various conditions, ice shape and what does it depend on, and to answer how will the change of pipe material affect the freezing? The subject of interest was also the determination of the thermal power of the pipes.

## 3. Methodology

Ansys-Fluent software can be used for solving fluid flow problems which involve processes of solidification and melting (SM). Software uses the Enthalpy-Porosity Technique [16] which is already widely used in many commercial codes [17] and well described in literature. This method was introduced by Voller and Prakash in 1987 to model phase-change in convection-diffusion problems [18]. In this technique phase front is not sharp and thus not tracked in explicit way. Instead of this, presence of a pseudo-porous medium called *mushy zone* is assumed between solid and liquid phase. *Mushy zone* occurs between *Liquidus* and *Solidus* temperatures which are start and end of solidification process – Liquidus is temperature at which material is completely liquid and Solidus states temperature at which material is fully solidified. In this region a quantity called *liquid fraction* $\beta$ varies between 1 (completely liquid) and 0 (completely solid). *Liquid fraction* indicates how much of the cell volume is in solid or liquid state – in other words *liquid fraction* represents porosity of the *mushy zone*. When material has fully solidified the velocities in material drops to 0, thus *mushy zone factor* $A_{mush}$ is introduced. It represents the rate of damping the velocities inside the material as it solidifies. The higher it is, the stronger the damping.

The energy equation used by SM solver is written as:

$$\frac{\partial}{\partial t}(\rho H) + \nabla \cdot (\rho \vec{v} H) = \nabla \cdot (k \nabla T) + S \quad (1)$$

where:

$H$ is enthalpy, [J], $\rho$ is density, [kg/m$^3$], $\vec{v}$ is fluid velocity [m/s], $S$ is source term.

Governing energy equation contains enthalpy of the material $H$ which is computed as a sum of sensible heat $h$ and latent heat $\Delta$H:

$$H = h + \Delta H \quad (2)$$

where:

$$h = h_{ref} + \int_{T_{ref}}^{T} c_p dT \quad (3)$$

$h_{ref}$ is reference enthalpy, [J], $T_{ref}$ is reference temperature, [K], $c_p$ specific heat at const. pressure, [J/kg*K].

Latent heat content $\Delta H$ depends on the *liquid fraction* $\beta$ and latent heat of the material $L$:

$$\Delta H = \beta L \quad (4)$$

Latent heat content varies between 0 for completely solidified material and L (for liquid).

*Liquid fraction* $\beta$ is defined as follows:

$$\beta = 0 \quad if \ T < T_{solidus} \quad (5.1)$$

$$\beta = 1 \quad if \ T > T_{liquidus} \quad (5.2)$$

$$\beta = \frac{T - T_{solidus}}{T_{liquidus} - T_{solidus}} \quad if \ T_{solidus} < T < T_{liquidus} \quad (5.3)$$

where:

$T_{solidus}$ is temperature at which material is completely solidified, $T_{liquidus}$ is temperature at which material is completely liquid.

To account for the velocity drop in a solid and for solid presence itself, sink terms are added to momentum and turbulence equation respectively.

Sink term for momentum equation is written as:

$$S = \frac{(1-\beta)^2}{(\beta^3 + \varepsilon)} A_{mush} \left(\vec{v} - \overrightarrow{v_p}\right) \quad (6)$$

where:

$A_{mush}$ is a mushy zone factor [N*s/m$^4$], $\beta$ is *liquid fraction* [-], $\overrightarrow{v_p}$ is pull velocity; velocity of solid which is pulled out of a domain – relevant for casting processes; in present case $\overrightarrow{v_p} = 0$, $\varepsilon$ is a small number 0.001 to prevent division by 0.

Sink term for turbulence equation is written as:

$$S = \frac{(1-\beta)^2}{(\beta^3+\varepsilon)} A_{mush} \varphi \qquad (7)$$

$\varphi$ = solved turbulence quantity (k, $\varepsilon$ $\omega$ and others; depending on the selected turbulence model)

To compute the temperature, an iteration between energy equation (1) and the *liquid fraction* equation (5.1-5.3) is executed. In Porosity-Enthalpy method, linear behavior of *liquid fraction* is assumed for temperatures between $T_{liquidus}$ and $T_{solidus}$.

From the point of view of the physics itself, Solidus and Liquidus for pure (one-component) substances like water or pure metals is the same. For alloys which contains different metals with different melting temperatures process of solidification and melting occurs in a range of temperatures ($T_{liquidus} \neq T_{solidus}$ ). In Fluent, in turn, based on these temperatures, the proportion of the liquid phase in a given cell is determined. In practice (even for pure materials), if *Liquidus* and *Solidus* temperatures are assumed the same, the shares of the liquid fraction would take only one of the two values: 0 and 1 in most of the domain (as in eq. 5.1-5.3), and it would change to the full extent only at temperature $T_{liquidus} = T_{solidus}$ which for water is at point 273.15. Thus, *mushy zone* would hardly develop at all, so it would solidify immediately, which would be not only unphysical, but also numerically unstable. Due to abovementioned nature of freezing numerical simulation - in this work $T_{liquidus} = 273{,}15\ K$ when $T_{solidus} = 272{,}85\ K$. This approach ensures a slight deviation of the model from the physical reality (exactly 0.3K) but allows to achieve more realistic results. Additionally, this approach was suggested by Ansys Support and was used in other works like in [10] and [11].

## 3.1 Numerical cases definition

**Numerical Case I** is a numerical, 3D steady simulation of the pipe made of high density polyethylene (HDPE) or aluminum through which the glycol flows. Pipe used in a Case I is a normalized PE-100 SDR17 32X2 PN10 pipe with an outer diameter of 32mm, inner diameter of 28mm, wall thickness of 2mm and length equal to 7.5m. Case I mesh contains 1.49 million elements and has been generated using only hexagonal elements which provided very high quality.

Outer surface of the pipe is at 0°C while ethylene glycol initial temperature is -20°C. The velocity of glycol is approximately 3.5 m/s. The use of such a pipe, the glycol temperature and the calculated glycol speed are the input data made available to the author of the work. Case I required to define HDPE properties [20,21] as well as a 40% ethylene glycol volume mixture with water. **HDPE thermo-physical parameters** for the sake of simplicity, were assumed constant for the entire temperature range were assumed and are as follows: Density $\boldsymbol{\rho}$ **=960 [kg/m$^3$]**, Specific heat ***Cp*= 1900 [J/kg*K]** and thermal conductivity $\boldsymbol{\lambda}$**=0.41[W/m*K].** For **aluminum** author used default and constant values defined in the software which are: Density $\boldsymbol{\rho}$ **=2719 [kg/m$^3$]**, Specific heat ***Cp*= 871 [J/kg*K]** and thermal conductivity $\boldsymbol{\lambda}$**=202.4[W/m*K].**
HTC value obtained numerically was additionally compared and successfully validated with the HTC value derived from Gnieliński's correlation.

Steady simulation was carried out using pressure-based solver with absolute velocity formulation and constant gravity acceleration equal to -9,81 m/s$^2$ along Z axis. Standard *k*-ε (2 eqn.) viscous model as an appropriate for turbulent flows was used with standard wall functions and default model constants. For pressure velocity coupling author used Coupled scheme. Numerical simulation was performed using default Coupled algorithm for pressure-velocity coupling and Rie and Chow distance-based flux type. For spatial discretization PRESTO! was used for pressure, while the Second Order Upwind algorithm was used for momentum, energy, turbulent kinetic energy and dissipation rate. Least Squares Cell Based method was used for calculation of gradients. Author used default under-relaxation factors which are: 0.5 for Pressure and Momentum, 1 for Density, Body Forces and Turbulent Viscosity, 0.75 for Turbulent Kinetic Energy, Turbulent Dissipation Rate and Energy. Default absolute convergence criteria were considered as sufficient and were set as 0.001 for continuity, velocities, *k* and ε, $10^{-6}$ for energy. The pseudo-time method and automatic time step were used in the calculations. The number of iterations was 400.

The heat transfer coefficient determined in Case I was the input value to the Numerical case II. Having HTC determined it allowed to remove glycol from the Numerical case II and replace it with a boundary condition of HTC and free stream temperature. Thanks to this, the Numerical case II was simplified.

**Numerical Case II** is a numerical, 2D transient simulation of water freezing around the cross section of the same pipe that was considered in Numerical Case I. Case II geometry is a cross-section of the pipe analyzed in Case I. Additionally, there is a cylindrical space filled with water around the pipe. The pipe has an outer diameter of 32mm, while the cylindrical area with water has a diameter of 150mm. The Case II mesh contains 76 800 elements and has been generated using only quad elements. Case II was developed in several variants (from A to E) with different boundary conditions to check as many physical conditions as possible that

may occur in the heat pump installation tank. Main assumptions of the variants are:

- **pressure outlet boundary condition** (named here as "open domain") in **Variants A and B** to allow exchange of the mass (backflow) at outer boundary of the fluid domain
- **wall type boundary condition** for the outer boundary of fluid domain in variants C, D, E (backflow not possible)
- use as a pipe material **HDPE** for variants **A, B, C, D**, and **aluminum** for variant **E**
- initial temperature of water and pipe for variants A, B, C, D, E as 10°C, 4°C ,0.05°C, 0.05°C and 0.05°C respectively
- Backflow temperature in A and B equal to initial water temperature
- for pipe inner edge a **boundary condition of free stream temperature equal to -20°C (**for all variants**)** and **HTC of 2005 [W/m$^2$K]** for **A, B, C**; **20050 W/m$^2$K** for **D** and **2044 W/m$^2$K** for **E**

Case II required the water to be user-defined material to best reflect its physical parameters that are key during cooling, convection, and freezing processes.

Transient simulation has been carried out on 2D planar space using pressure-based solver with absolute velocity formulation and constant gravity acceleration equal to -9,81 m/s$^2$ along Y axis. As described in Ansys Theory Guide only pressure based might be used in SM cases.

*Solidification and Melting (SM)* has turned on. SST k- $\omega$ (2 eqn.) viscous model has been chosen with Low-Re Corrections as for this process low values of Reynolds number were expected. For *SM* constant mushy zone parameter $A_{mush} = 10^7$ has been assumed. As this parameter is significant for process of shaping solid-liquid interface and for damping velocities in mushy region, it was found in literature, exactly in [10].
Numerical solution was performed using default Coupled algorithm for pressure-velocity coupling and Rie and Chow distance-based flux type. For spatial discretization PRESTO! was used for pressure, while the Second Order Upwind algorithm was used for momentum, energy, turbulent kinetic energy and dissipation rate. Least Squares Cell Based method was used for calculation of gradients. For transient formulation, Second Order Implicit Scheme was used for all simulations.
The time step for all simulations was fixed and equal to 0.1 s. The maximum number of iterations per step was 100.

## 4. Results and Discussion

All simulations were carried out until the author arbitrarily stated that their further continuation would not bring new conclusions and observations. For this reason, the time of individual simulations is different from each other.

The simulation results for all variants of Numerical Case II are included in Tables 1-4. While the liquid fraction and temperature contours are presented in figures 1-5. The analysis of the freezing process of all variants is supported by graphs and contours which are also analyzed.

Tab.1. Average liquid fraction in fluid domain.

| Case | II A | II B | II C | II D | II E |
|---|---|---|---|---|---|
| Time [s] | Liquid fraction | | | | |
| 0 | 1.0000 | 1.0000 | 1.0000 | 1.0000 | 1.0000 |
| 3600 | 1.0000 | 0.9983 | 0.9951 | 0.9947 | 0.9659 |
| 7200 | 0.9999 | 0.9853 | 0.9852 | 0.9834 | 0.9322 |
| 9000 | 0.9989 | **0.9848** | 0.9798 | 0.9776 | 0.9213 |
| 10800 | 0.9970 | | 0.9749 | 0.9725 | 0.9124 |
| 14400 | 0.9956 | | 0.9665 | 0.9638 | 0.8991 |
| 15600 | **0.9957** | | 0.9641 | 0.9613 | 0.8954 |
| 18000 | | | 0.9599 | 0.9572 | 0.8887 |
| 21600 | | | 0.9549 | 0.9521 | 0.8798 |
| 25200 | | | 0.9508 | 0.9480 | 0.8719 |
| 26100 | | | 0.9499 | **0.9470** | 0.8701 |
| 28800 | | | 0.9474 | | 0.8649 |
| 32400 | | | 0.9443 | | 0.8582 |
| 36000 | | | 0.9416 | | 0.8537 |
| 39600 | | | 0.9390 | | 0.8495 |
| 42000 | | | **0.9374** | | **0.8468** |

Tab. 2. Heat transfer rate on pipe outer edge.

| Case | II A | II B | II C | II D | II E |
|---|---|---|---|---|---|
| Time [s] | Total Heat Transfer Rate [W] | | | | |
| 300 | 145.94 | 408.32 | 339.39 | 371.09 | 2480.08 |
| 3600 | 470.90 | 333.78 | 326.71 | 356.00 | 1674.57 |
| 9000 | 373.18 | **308.41** | 318.03 | 344.96 | 1692.49 |
| 15600 | **380.88** | | 318.84 | 346.10 | 1783.98 |
| 26100 | | | 319.97 | **347.50** | 1782.07 |
| 42000 | | | **320.27** | | **1928.73** |

### 4.1 Case II A Analysis

Simulation A would be the starting point for a real phenomenon in the heat pump (water temperature typical for tap water) - i.e., the beginning of the heating season. Ice build-up is very small and concentrated in two 'bubbles' symmetrically positioned a bit to left and a bit to right from the bottom of the pipe surface. No ice has formed on the top and side edges of the pipe. The reasons for such

a formation of ice are to be found in the nature of the water flow around the pipe (not visible at the contours). It was flow from top to bottom, maintained throughout the whole simulation. It caused also developing of an area of stagnant water with the lowest temperature (fig.1b) is created under the pipe, washed on the left and right with a stronger current of water

Practically, this means that in the initial period of the heat pump operation, an increase in ice can be expected only where the water has a sufficiently long contact time with the pipe - i.e., in its lower part. The simulation was stopped at 15600s because the liquid fraction stopped decreasing and even started to delicately fluctuate. The open boundary of the domain caused cold water to run out and constantly replace it with warmer water - this has led, so to speak, to create a pseudo steady state and it is physical reason for mentioned fluctuations. In this state, the heat taken up by the glycol comes not from the water that is in the domain, but from the water outside the domain. This results in little or no ice gain and no new observations within the domain. In reality, however, it would lead to a gradual and even cooling of the water in the tank, which, for the analyzed situation, would mean a gradual decrease of backflow temperature over time. This means that until the global temperature of the water in the reservoir decreases, no more ice will appear.

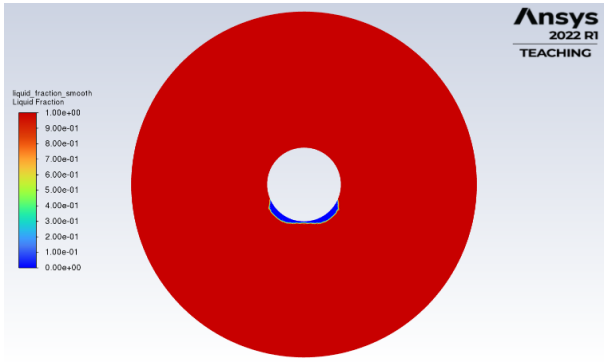


Fig. 1a Case II A liquid fraction at 15600s.

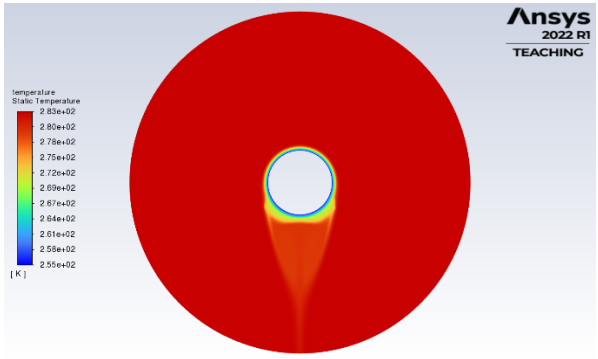


Fig.1b Case II A temperature at15600s.

## 4.2 Case II B Analysis

In simulation B the greatest increases in ice were observed in the middle and lower parts of the side edges of the pipe, although initially the ice began to grow on the upper edge of the pipe (not visible here). At the beginning of freezing the upward movement of the water was visible at the top of the pipe. Then, the downward movement of the water begins to dominate in the entire domain, suppressing the upward movement of cooler water.

The increase in the velocity of the water around pipe pushed the previously cooled water from the top region downwards causing it to cool further and, consequently, to form ice around the side edges of the pipe.

Next, the ice was growing only in width, a thin layer of ice was kept at the very bottom of the pipe, while the main increase occurred horizontally, symmetrically on both sides of the pipe. Within the progress of simulation time, similarly to the model II A, an almost stationary area of water developed under the pipe. The simulation has been stopped after 9000s as the rate of ice growth began to slow down significantly and its nature remained unchanged. As in the case of IIA, the simulation practically stood still and there was no need to continue it. Considering the puzzling nature of the obtained ice shape (it seems to grow in non-physical way), it can be concluded that in the case of water with a temperature of 4 degrees, the greatest ice growth should occur on the sides of the pipe. Finally, the lack of ice in the upper part of the pipe requires rethinking the correctness of the model in terms of backflow definition and maybe the size of the domain (perhaps it was too small to accurately reproduce very subtle convection movements).

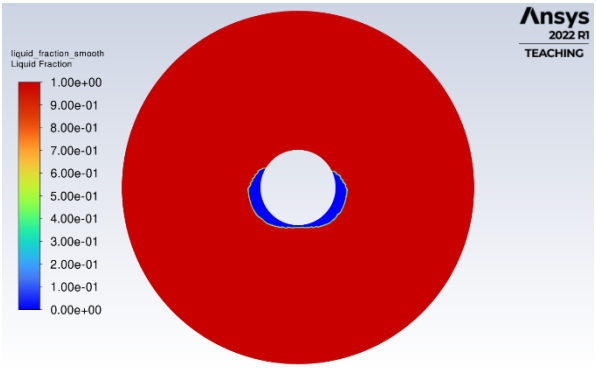


Fig. 2a Case II B liquid fraction at 9000s.

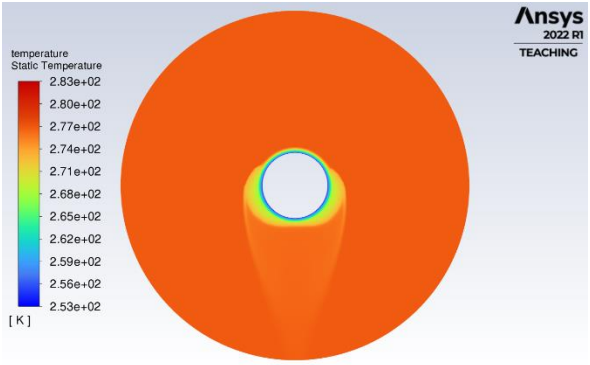


Fig. 2b Case II B temperature at 9000s.

## 4.3 Case II C Analysis

The II C simulation was an attempt to obtain as much ice as possible due to small ice increments in simulations A and B. An attempt was made to achieve this by domain closure (changing the boundary condition from pressure outlet to wall) and by setting up initial water temperature of 0.05°C. As such a change causes an obvious distortion of water movements around the pipe, it was found that in this and subsequent cases the most important is a change in the *liquid fraction* in the entire domain, not the shape of the ice formed. The contours show a clear tendency for ice to grow at the bottom edge of the pipe. In the initial phase of the simulation, the pipe was covered with an even thin layer of ice, and after that ice starts to grow mainly at the bottom, changing its shape from a relatively wide "cornice" to an increasingly elongated drop / icicle. Interestingly, in the remaining space of the domain the water was freezing very evenly - the liquid fraction gradation practically did not occur, and the value of this parameter was almost independent of distance from the pipe. Only the area at the very bottom of the domain was filled with completely liquid water (*liquid fraction* =1). Very slow and even freezing in the area outside of fully solid ice leads to the production of a poorly developed *mushy zone* - it fact, it would be a mixture of water and ice particles, or just a kind of "ice slurry". In this area, a strong damping of velocity was observed (having $A_{mush}=10^7$ as assumed before, just the *liquid fraction* value of ~ 0.95 causes almost complete cessation of convective movements). The simulation lasted 42,000 s and was stopped as before when the change in *liquid fraction* slowed down significantly, and the nature of the changes was still the same. The variant II C proves that even in very favorable conditions to freezing, the ice growth is again very small.

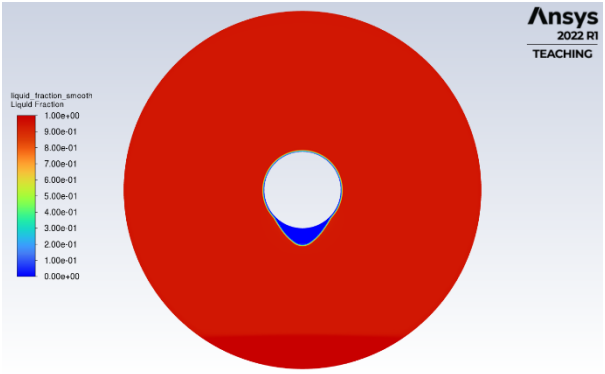


Fig. 3 Case II C liquid fraction at 42000s.

## 4.4 Case II D Analysis

A simulation of the II D variant was performed to confirm the observations of the IIC variant. In this case, the heat transfer coefficient was artificially increased 10 times. This would correspond to an increase in pipe velocity to around 60 m/s (calculated from Case I). This value is non-physical and cannot be obtained in the heat pump installation. As the results in IID are very similar to IIC, the fact of having very high value of HTC clearly shows that even by increasing the speed and thus the volumetric flow rate of refrigerant, it is not possible to sensibly improve the freezing conditions while using HDPE pipes. Analyzing the shape of the ice and the course of the process it must be said that way of freezing is almost identical to one in variant II C. The only difference is that process is slightly accelerated (especially in the initial phase Therefore, artificially increasing the heat transfer coefficient did not give any practical effect. Simulation was stopped after 26100s.

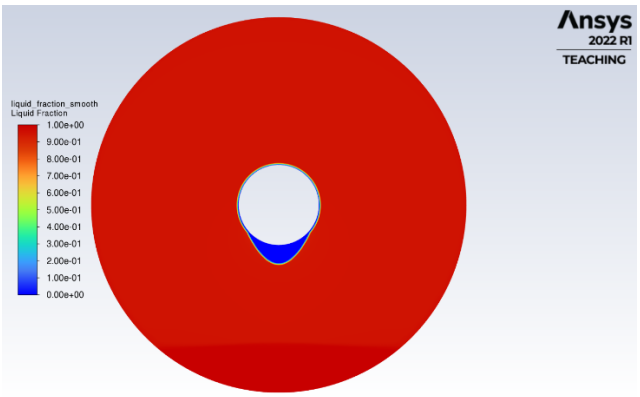


Fig. 4 Case II D liquid fraction at 26100s.

## 4.5 Case II E Analysis

The course of the simulation, as expected, was characterized by the fastest rate of ice growth. At first, the pipe was covered with a thin layer of ice around it, while its main growth took place in pipe's bottom part. A very wide icicle was created, with a

width greater than the diameter of the pipe. As the simulation advance, the ice slurry region (an area freezing evenly with a fairly high *liquid fraction*) was more visible. With the progress of simulation this area took up more and more of the domain, leaving fully liquid water only at the bottom. What is intriguing, however, this time the mentioned slurry region does not reach as low as in the previous simulations - the *liquid fraction* drops faster than before, while the bottom edge of the region is always a bit above the bottom edge of the fully solidified icicle. Additionally, what is the most evident in case IIE, is the complete disappearance of velocity within even poorly developed *mushy zone*. The simulation was run until 42000s corresponding to the IIC simulation. Further progress was possible however more significant results would be possible after a very long time..

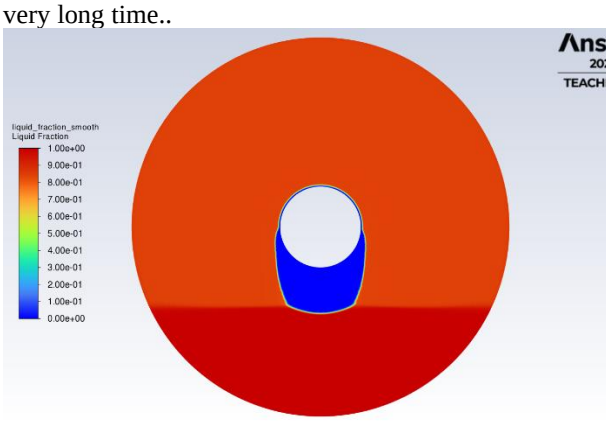


Fig.5 Case II E liquid fraction at 42000s.

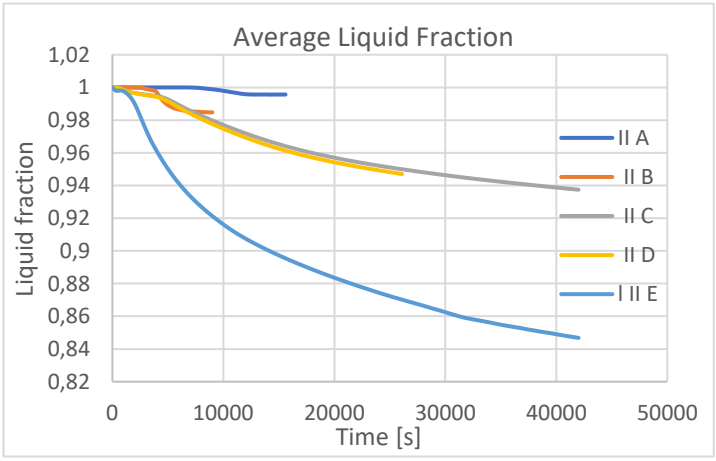


Fig. 6 Average liquid fraction for all variants

In all cases, a cooling period can be distinguished, in which freezing does not occur. For cases with lower starting temperature of water, it is obviously shorter. Another characteristic feature of all simulations is the gradual decrease in the freezing speed - the graphs flatten. Simulations A and B with an open liquid domain relatively quickly reach a state where freezing slows down almost completely. From a practical point of view, this suggests that, at least when HDPE is used as a pipe material, it will initially grow with a small layer of ice, which will only start to build up again when the surrounding water has cooled sufficiently.
IIC, IID and IIE simulations do not show such a drastic slowdown in freezing as in A and B, because the cooled liquid does not flow out of the domain.

## 4.5 Time estimations

Tab. 3. Estimated, lower time limit of full freezing.

| Time to full solidification (lower limit) | | | | | | |
|---|---|---|---|---|---|---|
| Case | Rate of last 60min | | | Rate of last 30min | | |
| | hours | days | R2 | hours | days | R2 |
| IIA* | 5582.17 | 232.59 | - | - | - | - |
| IIB | 375.72 | 15.65 | 0.851256 | 916.21 | 38.18 | 0.968954 |
| IIC | 401.98 | 16.75 | 0.999894 | 409.61 | 17.07 | 0.999969 |
| IIC* | 251.38 | 10.47 | - | - | - | - |
| IID | 246.18 | 10.26 | 0.999652 | 254.64 | 10.61 | 0.999896 |
| IIE | 219.56 | 9.15 | 0.999601 | 226.09 | 9.42 | 0.999606 |

Based on the rate of ice growth in the last 60 and 30 minutes of each simulation, it was estimated how much theoretically it would take for the entire domain to fully freeze out. Results are presented in table 3. This estimation was made by fitting the linear trendline to the last 30/60min segment of the *liquid fraction* function. A linear trendline was chosen as it indicated the most probable results. The liquid fraction function is not linear throughout its full course, however, the most important thing in estimating the time of full freezing is its final fragment - there is certainly no way that freezing would start to accelerate, or after such a long time it would change its character radically. Therefore, freezing will proceed at the same (rather unlikely) or slower rate in approximately linear way. In that case, logarithmic or polynomial trend functions gave a good fit in the full range of graph functions, while they yielded completely absurd results in the predicted area. Linear functions, although they assume maintaining a constant freezing rate, give at least an approximate result as to how long the process can still go on (i.e., exactly when the $\beta = 0$ condition is met). Therefore, the author is aware that the estimated freezing times should be treated very indicatively – they constitute for lower limit of full solidification.

The results in Table 3 show that in every case the time needed to complete the simulation (reach $\beta = 0$) would be counted in many days. The time in the case of IIA due to the weak fit of the trend line was calculated based on the change in *liquid fraction* in the last hour without creating a linear function. The

final value of the *liquid fraction* was divided by the change that occurred in the last hour of the simulation, obtaining the number of hours needed to complete the simulation. After adding the time of the already recalculated simulation, the obtained result gave the theoretical, minimum time of full freezing Such a method gave practically the same results as the approximation with a linear function, provided that the determination coefficient was high. The IIC* estimated time was calculated in the same way, which corresponds to the change in liquid fraction in the range 22500-26100s, i.e. the last hour of the IID simulation. From this, it is clear, that at the corresponding times, the IIC and IID simulations had almost the same freezing rate. Obtained estimated times differ depending on the adopted range - the difference between the rate of the last 30/60 minutes is very visible in the case of IIB. In the case of IIA, over the last 30 minutes, the function had been increasing so any estimation was meaningless. In the cases IIC, IID and IIE the differences are small indicating a very slow inhibition of freezing. Approximated times of full solidification (which in fact would be greater because the freezing rate would continue to fall) suggest that calculating any variant to the end was technically impossible. The calculations of the model II took the author 2 months - during this time the simulations were running practically non-stop 24 hours a day.

## 4.6 Pipe Resistances

The obtained simulation results lead to an important question - Why increasing the heat transfer coefficient on the glycol side (i.e., in fact increasing its velocity and volumetric flow rate) did not give any noticeable change, while the change of material multiplied the rate of ice growth? For this purpose calculated the thermal resistance of considered pipes.The given resistances in that situation can be calculated from the equation:

$$R_{total} = R_{conv,1} + R_{cyl} + R_{conv,2} \quad (8)$$
$$= \frac{1}{(2\pi r_1 L)\cdot HTC_1} + \frac{\ln\left(\frac{r_2}{r_1}\right)}{2\pi L\lambda} + \frac{1}{(2\pi r_2 L)\cdot HTC_2}$$

where: $HTC_1$, $HTC_2$ are heat transfer coefficients on inner and outer side of the pipe, λ is thermal conductivity of the pipe material and L is pipe length.
Assuming L = 1m, we obtain the resistance for a one running meter of the pipe. We can insert the resistances obtained in this way into the next equation:

$$\dot{Q} = \frac{\Delta T}{R_{conv,1} + R_{cyl} + R_{conv,2}} \quad (9)$$

where: Q is total heat transferred in [W] and ΔT is temperature difference in [K] between fluids inside and outside the pipe.

Tab. 4 Pipe Resistances

| Pipe's thermal resistance | | | | | |
|---|---|---|---|---|---|
| Variable | Unit | HDPE | Aluminium | % of Rc total | |
| HTC1 (α1) | W/m2*K | 2005 | 2044 | | |
| λ | W/m*K | 0,41 | 202,4 | | |
| HTC1 (α2) | W/m2*K | 2023 | 1834 | HDPE | Aluminium |
| $R_{conv,1}$ | K/W | 0,00566993 | 0,005561747 | 9,08 | 50,15 |
| $R_{\lambda}$ | K/W | 0,05183459 | 0,000105001 | 83,04 | 0,95 |
| $R_{conv,2}$ | K/W | 0,00491705 | 0,005423764 | 7,88 | 48,90 |
| $R_{total}$ | K/W | 0,06242156 | 0,011090512 | Values in the table are calculated for t=26100s for Variant C and Variant E. | |
| $\dot{Q}$ | W / running meter | 319,96 | 1782,07 | | |
| Pipe Length to reach 1kW power | m | 3,13 | 0,56 | | |

For both HDPE and aluminum, the heat transfer coefficient on the water side is as high or even slightly higher than on the glycol side. Apparently, this may appear to be too high for natural convection. However, value of $HTC_2$ is also affected by the freezing process so it might be higher than expected. The presented thermal resistances show that the conduction resistance has the main influence on the heat transfer rate. This ultimately results in about 5.5 times greater total thermal resistance of pipes made of HDPE compared to pipes made of aluminum. Convection resistances for both materials on both the glycol and the water side are similar to each other. Their total value for HDPE is about 17% of the total resistance, while for aluminum it is 99%. These results explain the very minor change in the ice growth rate in simulation D versus C. For HDPE pipe, the thermal resistance on the coolant side is only 9% of the total resistance, while for aluminum it is 50%. This suggests a much better control of the freezing rate by changing the glycol flow rate for aluminum pipes. At the same time, it shows reverse tendency in case of HDPE pipes - even a very large and technically impossible increase in HTC1 (i.e., in practice the glycol flow rate) at the HDPE pipe gives little effect - the heat transfer rate increased by about 8.5% to 347.5 W (compare with table 2). Finally, length of pipes needed to obtain 1kW of power - for aluminum it is only 0,56m, while for HDPE it is about 5,5 times more - 3.13m.

## 5. Conclusions

The aim of the work was to check some technical assumptions made by a company that wanted to build heat pump installations with a water reservoir in the future. These assumptions concerned

the pipe material used (HDPE) and the very idea of conducting freezing through a set of many, long spirals made of such pipes through which ethylene glycol flows.

In the work, it was possible to successfully determine ice growth rate in several cases and to check the efficiency of heat transfer and its consequences for two completely different materials. The qualitative analysis of the ice shape suggests the necessity to conduct empirical experiments or to optimize the model settings. Unfortunately, with the previously mentioned computing powers and very long calculation times, it was impossible to analyze more complex cases or to calculate to the end the cases from this thesis. Therefore, it was impossible to accurately capture the more comprehensive convective movements that could occur in the heat pump's tank, and which thus determine the shape of the obtained ice.

The results obtained in the thesis suggest that the use of HDPE as a pipe material is questionable. It is a cheap material but at the same time it has very poor thermal conductivity. The quantitative assessment of the ice growth during the simulation shows that there are 2 possible approaches: the pipe material should be a metal with a good thermal conductivity, e.g., aluminum or, to obtain the same power, it would be needed to use longer HDPE pipes.

While using HDPE pipes installation would probably be very simple and rather cheap, because this kind of pipes are easy to assembly. To obtain the desired power, 3.13m of the pipe is needed for every 1kW. Due to slow increase in glycol temperature of about 0.046 K/running meter, in the case of HDPE, the desired power can actually be obtained from a long loop (even several dozen meters). The longer the loop, the greater will be the difference between the amount of ice formed around the pipe at the beginning and end of the loop and thus heat transfer rate will decrease along the length of the pipe. For HDPE, this difference will be small. Assuming that calculated increase in average glycol temperature is constant and uniform conditions around the pipe, the maximum length of a single loop would be 434.8m. Above this value, the glycol would be above 273.15K and freezing would be impossible.

Installation with HDPE pipes would have little control possibilities resulting from the poor thermal conductivity of HDPE, which reduces the effectiveness of glycol flow rate control. In the case of HDPE, the desire to improve the heat transfer conditions could be by using composites of HDPE and expanded graphite (EG) that are originally prepared for heat exchangers in multi-effect distillation. In a paper [26] authors claim that one of the plasmas treated HDPE/EG composite had overall heat transfer coefficient of about 98% that of stainless steel.

Making pipes of aluminum would on the other hand reduce both the loops length and the energy consumption needed to pump the refrigerant but at the same time would increase construction costs as aluminum is more expensive and fur sure more demanding in case of montage and forming desirable shapes and connections. To obtain 1kW pipe needs to be only 0.56m long. The increase in the average glycol temperature in the aluminum pipe was 0.51 K/running meter. With the same assumptions as before, the maximum length of the aluminum pipe above which freezing stops is 39.22m. These results lead to the conclusion that in case of aluminum there is need to create shorter (and thus probably more) loops (otherwise there will be large differences in ice growth between the beginning and end of a given loop). The use of aluminum provides excellent process control capabilities by varying the volumetric flow of the glycol. Thanks to this, it will be possible to save energy used to pump the cooling medium, because to reach same heat transfer rate like in HDPE case would mean to pump less medium at a lower speed.

When considering the possible layout of pipes in the tank, it is worth mentioning one issue here. The distribution of pipes in the tank should be as even as possible and leave no larger spaces between them. The required number of pipe loops should depend on the required power, the length constraints mentioned before and on the volume of the tank. It is impossible to allow a situation in which the tank is not adjusted to the heat exchanger - it may cause the undesirable nature of ice growth, i.e., its unfavorable shape, distribution, and quantity.

As for the technological problems with ice build-up, they should not occur at least until all the water in the tank has cooled to a temperature close to freezing point – this was proven by simulations IIA and IIB where ice buildup stopped after few hours forming minor amounts of ice. Ice accumulation is strongly inhibited by movements of water with a temperature higher than its freezing temperature. For a long time of use of the heat pump, the pipes will be only partially covered with ice until the water temperature drops to around 0°C.

As a recommendation - freezing process should involve the formation of ice from the bottom to the top, possibly without water pockets bounded by ice walls. Larger amounts of ice are desirable only at the end of the heating season, when we want to accumulate as much ice as possible for the summer - until then, if it’s possible and necessary, heat regeneration should be used.

The qualitative analysis of the ice, i.e., its shape and how it grew during the simulation, brings conclusions that, according to the author, are partially puzzling. The problem is the mapping of convective movements around the pipe – in simulations A and B, it is quite unexpected that the liquid moves from the top to the bottom of the

domain. For those who want to deal with the problem of simulating freezing around pipes in the future, the author recommends carefully studying and testing the pressure outlet boundary condition and backflow options. These two things and the matching of a sufficiently large computational domain would certainly allow to better reflect the nature of the very subtle movements of natural convection taking place in the tank. In this situation, it is also necessary to carry out validation experiment. It would be very helpful to check how the ice actually grows. Performing such an experiment could also allow to find more optimal settings for the solidification and melting module. As stated in [10], $\Delta T_m$ and $A_{mush}$ are not independent of each other. In this work, the author used the suggested values found in scientific articles that dealt with the topic of freezing of water under natural convection conditions. Perhaps, however, after conducting the experiment, these assumptions might be corrected for the purpose of further work in this field.

2D simulations have shown how complex and sensitive the freezing process is, even when using very simple geometry. Based on the obtained results, it is difficult to conclude what would be the optimal distribution of pipes or the shape of the heat exchanger for the type of installation analyzed in this work. As can be seen, the nature of the water's convective movements is of key importance for the shape of the growing ice. Correct mapping of these movements in the numerical simulation and the analysis of their consequences is, according to the author, the most important for the correct design of the heat exchanger in the water tank. By analyzing several Numerical Case II variants, an attempt was made to replicate plausible and relevant freezing conditions. To fully investigate the phenomenon, several more analyzes should be carried out, the lack of which, unfortunately, makes it impossible to fully answer the question of how to arrange the pipes in the tank. According to the author of the work, subsequent 2D simulations should test how it will affect the freezing of several (at least 4-6) pipes next to each other – preferably in different geometric configurations. A step further would be a 3D simulation. A simulation containing more pipes would allow to learn more about how the water movement in the reservoir changes under the influence of not one, but several sources of cooling, and thus find the optimal configuration of their arrangement. A 2D analysis of only one pipe can only be used as a guide.

The conclusion of this work is the confirmation of the necessity to use significant computing resources for solidification and melting simulations

Assuming the correctness of the obtained results, it should be suggested that the pipes in the heat exchanger in the water tank should not be placed directly underneath the other – in such a configuration, ice growing mainly downwards would connect the pipes leaving more unfrozen water between them.

Even when creating very favorable conditions for freezing (aluminum pipes), the process takes place slowly – the surrounding of the pipe needs at least around 9 days to freeze the entire cylindrical volume with a diameter of 15 cm.

The final conclusion from this thesis is the recommendation to avoid icing the pipes as long as possible in this type of installations. The production of ice is not an end in itself – it allows to draw more energy from a finite volume of water, additionally receiving a source of coolness for the summer season. However, it should be avoided as long as possible as ice deteriorates the heat transfer between pipes and water. Only in the final phase of the heating season it will be desirable to obtain large amounts of ice.

## 6. References


[1] Heat pump, https://en.wikipedia.org/wiki/Heat_pump

[2] Gutkowski K., Butrymowicz D. et al. „Chłodnictwo i Klimatyzacja w. 4*", ISBN: 978-83-01-21345-9, 2022*

[3] Types of heat pumps, https://www.linquip.com/blog/types-of-heat-pump/

[4] Ansys, Inc. "Ansys Fluent Theory Guide 2022 R1", January 2022

[5] Faden M., König-Haagen A., Brüggemann D., "An Optimum Enthalpy Approach for Melting and Solidification with Volume Change", *03.2019 Energies MDPI Journal*

[6] V. R. Voller and C. Prakash. "A Fixed-Grid Numerical Modeling Methodology for Convection-Diffusion Mushy Region Phase-Change Problems". *Int. J. Heat Mass Transfer*. 30. 1709–1720. 1987.

[7] Dallaire J., Gosselin L., "Numerical modeling of solid-liquid phase change in a closed 2D cavity with density change, elastic wall and natural convection", *International Journal of Heat and Mass Transfer 114 (2017) 903–914*

[8] Asip Khan L. Mahabat Khan M., "Role of orientation of fins in performance enhancement
of a latent Thermal Energy Storage Unit", *Applied Thermal Engineering (2020)*, doi: https://doi.org/10.1016/j.applthermaleng.2020.115408
[8] Bourdillon A.C., Verdin P.G., Thompson C.P., "Numerical simulations of water freezing processes in cavities and cylindrical enclosures", *Applied Thermal Engineering 75 (2015) 839-855*

[9] High-Density Polyethylene,

https://polymerdatabase.com/Commercial%20Polymers/HDPE.html

[10] Thermal Properties of Plastic Materials, https://www.professionalplastics.com/professionalplastics/ThermalPropertiesofPlasticMaterials.pdf

[11] Patrik Sobol˘ciak , Asma Abdulgader et al. "Thermally Conductive Polyethylene/Expanded Graphite Composites as Heat Transfer Surface: Mechanical, Thermo-Physical and Surface Behavior" *11.2020, Polymers MDPI Journal*